

**Modelling the  
bidirectional reflectance  
distribution functions  
(BRDF) of sea areas  
polluted by oil**

OCEANOLOGIA, 46 (4), 2004.  
pp. 505–518.

© 2004, by Institute of  
Oceanology PAS.

**KEYWORDS**

Reflectance  
BRDF  
Remote sensing  
Radiance

ZBIGNIEW OTREMBA

Gdynia Maritime University,  
Morska 83, PL-81-225 Gdynia, Poland;  
e-mail: zotremba@am.gdynia.pl

Manuscript received 8 July 2004, reviewed 30 August 2004, accepted 22 September 2004.

**Abstract**

The paper discusses the possibilities of modelling the bi-directional reflectance distribution function (BRDF) in sea areas polluted by oil. Three sea basin models are considered: a coastal one free of oil, one polluted by an oil film and one polluted by an oil emulsion. The following concentrations of oil were compared: for the film, 1 cm<sup>3</sup> of oil per 1 m<sup>2</sup> water surface, for the emulsion 1 cm<sup>3</sup> of oil in 1 m<sup>3</sup> of water. The optical properties of *Romashkino* crude oil were taken into consideration, as were various angles of incident solar light. The conversion of BRDFs into a directional distribution of the optical contrast of polluted areas is demonstrated.

**1. Introduction**

Oil pollution in the sea is a very serious problem for both the petroleum industry and the management of the marine environment. Oil-stress indicators have therefore been established for selected marine areas. For example, in the Baltic Sea, the HELCOM indicators are the number and size of spillages detected every year thanks to international air surveillance with remote sensing equipment (HELCOM 1991). So far, a total of almost 900 spillages have been recorded in the Baltic and North Sea areas covered by aerial inspections (HELCOM 2002). At the same time it should be

The complete text of the paper is available at <http://www.iopan.gda.pl/oceanologia/>

mentioned that aerial inspections are suitable for detecting surface forms of oil (films), whereas immersed forms are invisible to current remote sensing equipment.

There are a number of ways in which the optical phenomena generated by oil in the sea can be analysed. The principal questions relate to the detection of oil pollution, the form that such pollution takes, the concentration or overall mass of oil, and the estimation of the spatial extent of the polluted sea area. The impact of various forms of oil on reflected light is also important for the remote sensing of aquatic environments. The possibilities of detecting oil immersed in the sea by methods other than optical ones are poor, since only visible light can relatively easily penetrate water; if the sea water contains an additional oil emulsion, the diffuse component of the water radiance field is modified.

Both factors – the oil film and the oil-in-water emulsion – can be investigated as modifiers of this water light field by the use of the Monte Carlo method. This has become possible since the optical features of oil films and emulsions can now be quantified. It has been found that oil films on the water surface are optically represented by the following four functions: they are the angular distributions of transmittance and reflectance, separately for the upward and downward directions (each function for a definite wavelength and oil film thickness) (Otremba 2000). However, oil emulsions are represented by two quantities: the absorption coefficient  $a$  and the volume scattering function  $\beta(\theta)$  (the scattering function  $\beta(\theta)$  is usually represented by two quantities: the scattering coefficient  $b$  and the phase function  $p(\theta)$ ). As far as remote sensing is concerned, the complete optical characteristics of both land and sea areas are given by the bi-directional reflectance distribution function (BRDF). The BRDF is a strictly defined, inherent optical quantity that allows the reflected radiance field to be calculated, which for a particular wavelength is expressed by integral (1), in which the BRDF is denoted by  $f_r(\theta_i, \varphi_i, \theta_r, \varphi_r)$ .

$$L_r(\theta_r, \varphi_r) = \iint_{00}^{2\pi \frac{\pi}{2}} f_r(\theta_i, \varphi_i, \theta_r, \varphi_r) L_i(\theta_i, \varphi_i) \sin \theta_i \cos \theta_i d\theta_i d\varphi_i, \quad (1)$$

where

- $L_r(\theta_r, \varphi_r)$  – reflected radiance,
- $r(\theta_i, \varphi_i, \theta_r, \varphi_r)$  – BRDF,
- $L_i(\theta_i, \varphi_i)$  – incident radiance,
- $\theta_i$  – nadir angle for incident photons ( $0 < \theta < \pi/2$ ),
- $\varphi_i$  – azimuth angle for incident photons,
- $\theta_r$  – nadir angle for reflected photons ( $\pi/2 < \theta < \pi$ ),
- $\varphi_r$  – azimuth angle for reflected photons.

The BRDF definition was first put forward by Nicodemus (1963, 1970, 1977) to describe the optical features of a land area. This concept and its methodology have since undergone considerable development (Martonchik et al. 2000). In recent years the BRDF has also been applied to the characterisation of marine areas (Otremba 2002, Mobley et al. 2003). Preliminary tests were carried out to include the BRDF in operational satellite activity (Liang & Strahler 1999, Schaaf et al. 2002). Unfortunately, the BRDF is very hard to measure directly in an aquatic environment, but there is a possibility of modelling the BRDF using the Monte Carlo method, if the inherent optical parameters of all the dissolved and suspended components of waters (IOPs) are known.

Oil is a substance that can persist in the marine environment for a long period of time. It was chosen for the present study, because it is by volume the greatest single source of pollution in seas and oceans, the input of which is estimated at millions of tonnes per year (NRC 2003).

### Models of the environments studied

Three environmental models were used. The first one (Fig. 1a) was a coastal sea area in which the optical parameters of case II water were applied. Real values of IOPs appropriate to the Gulf of Gdańsk (southern Baltic Sea) for the middle of the visible spectrum ( $\lambda = 550$  nm) were taken: the absorption coefficient  $a = 0.3 \text{ m}^{-1}$  and the scattering coefficient  $b = 0.5 \text{ m}^{-1}$ . The phase function of light scattering  $p(\theta)$  (after Petzold 1977) was applied: two quantities – the scattering coefficient  $a$  and the phase function  $p(\theta)$  – replaced the volume scattering function  $\beta(\theta)$ . The second model

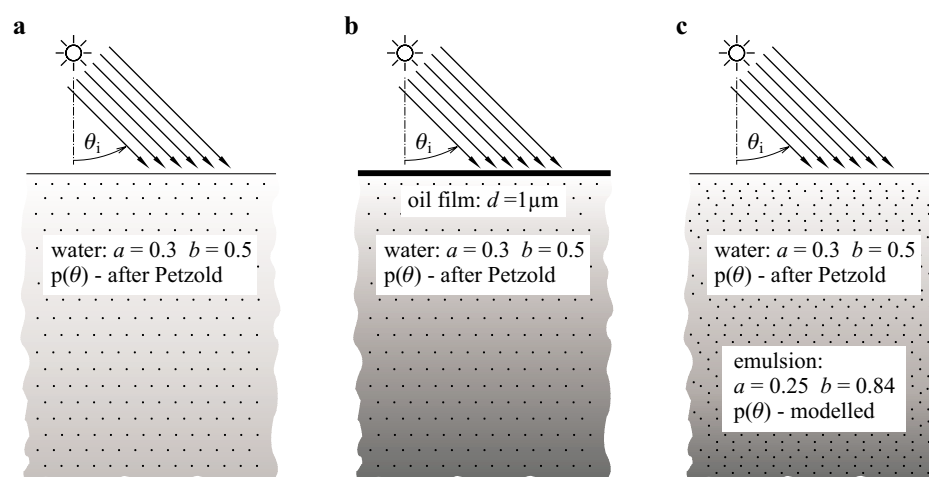
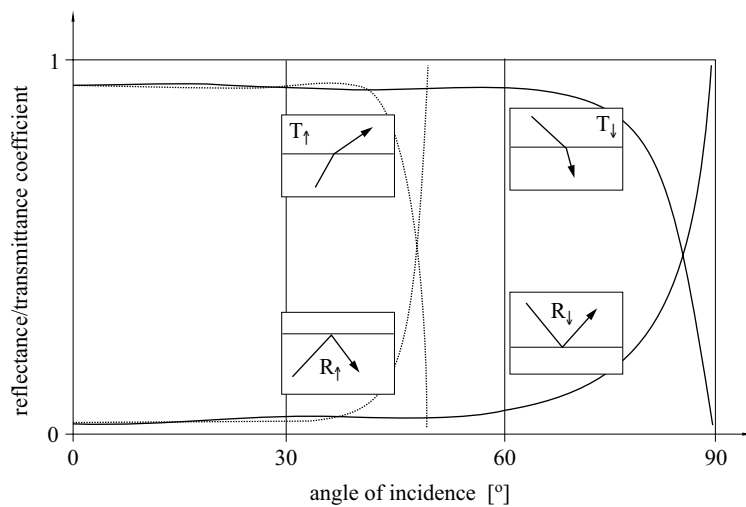
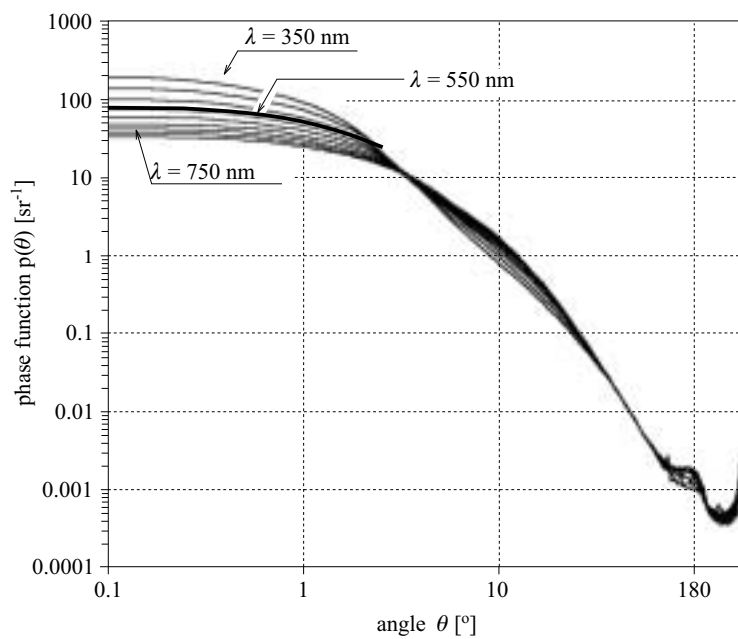


Fig. 1. Models of the environments studied



**Fig. 2.** Angular dependencies of the optical features of a 1  $\mu\text{m}$  thick oil film floating on a sea water surface for wavelength  $\lambda = 550 \text{ nm}$



**Fig. 3.** Phase functions of an oil-in-water emulsion (*Romashkino* crude oil in sea water). Curves for wavelengths from 350 nm to 750 nm every 50 nm (thick line for 550 nm)

(Fig. 1b) was the same as the first one, except that the water surface was covered by an oil film 1  $\mu\text{m}$  thick. The oil film was of *Romashkino* crude oil (the optical properties of this oil are similar to those of most oils). The optical properties of such an oil film have been published (Otremba 2000): the real part of the refractive index  $n = 1.488$ , the imaginary part of the refractive index  $k = 0.004$ , the angular dependencies of the reflection coefficients ( $R \downarrow$ ,  $R \uparrow$ ) and transmission coefficients ( $T \downarrow$ ,  $T \uparrow$ ) are presented in Fig. 2. The third model (Fig. 1c) was also like the first, but the water was polluted by an oil emulsion produced from the same oil as in the second model. The optical features of this oil-in-water emulsion were: absorption coefficient  $a = 0.25$ , scattering coefficient  $b = 0.84$ , phase function of light scattering  $p(\theta)$  (Fig. 3) cited after Otremba & Piskozub (2004).

In all cases the sea surface was flat, and the sea was sufficiently deep (100 m) for the radiative transfer to remain unaffected by the seabed.

### Monte Carlo model settings

The solar incident irradiance was represented by 1 billion virtual photons incident on the sea surface under a given angle  $\theta_i$ . The upper hemisphere was covered by one thousand eight hundred and thirty-three virtual receivers of photons, including photons entering solid angles of various values. One thousand two hundred and ninety-six receivers captured photons in sectors 0.004363323130 sr in size; 252 receivers were 2.5 times smaller, 144–5 times smaller, while 144 were closest to the zenith sectors, which were 10 times smaller in size.

## 2. Results

Simulations were carried out for 5 directions of solar light incidence  $\theta_i$  ( $0^\circ$ ,  $20^\circ$ ,  $40^\circ$ ,  $60^\circ$ ,  $80^\circ$ ), separately for a sea area free of oil, for a sea area polluted by an oil film, and for a sea area polluted by an oil-in-water emulsion (15 cases in all). The output data of the simulations are  $51 \times 36$  matrices (51 nadir angles, 36 azimuth angles). The step method for smoothing all the matrices was applied. Examples of a raw matrix and a smoothed one are illustrated in Fig. 4. All matrices were developed so as to present them in cylindrical coordinates in which the radius coordinate is a nadir angle and the azimuth coordinate is an azimuth angle. The results shown in Fig. 4 in Cartesian coordinates are replicated in Fig. 5 in cylindrical coordinates, which are more suitable for BRDF visualisation.

The BRDFs for four azimuth angles  $\varphi_r$  were extracted from the output matrices in pairs as follows:  $0^\circ$  &  $180^\circ$ ,  $30^\circ$  &  $210^\circ$ ,  $60^\circ$  &  $240^\circ$  and  $90^\circ$  &  $270^\circ$ .

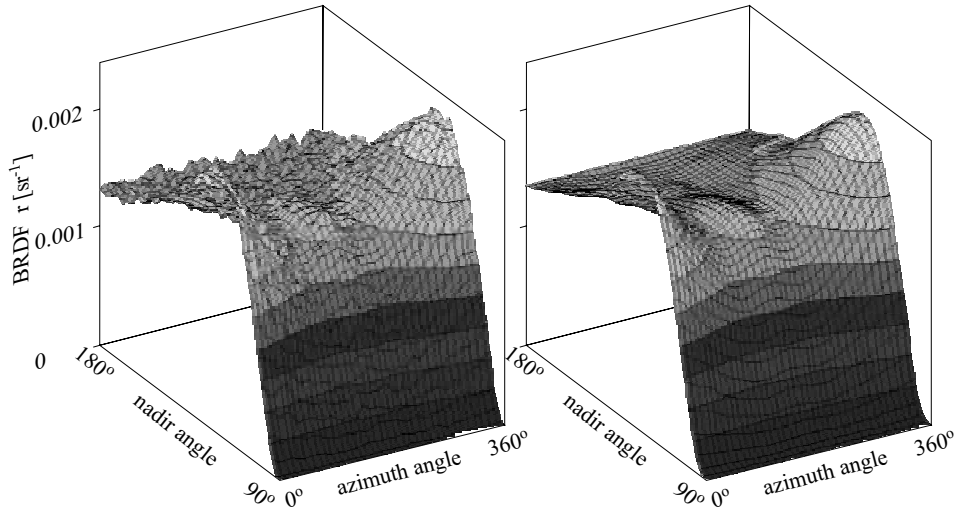


**Fig. 4.** Illustration of the BRDF output matrix before (left) and after smoothing (right). This example refers to the BRDF of the sea area covered by an oil film (thickness  $1 \mu\text{m}$ ) for solar illumination incident at the angles  $\theta_i = 30^\circ$ ,  $\varphi_i = 0^\circ$

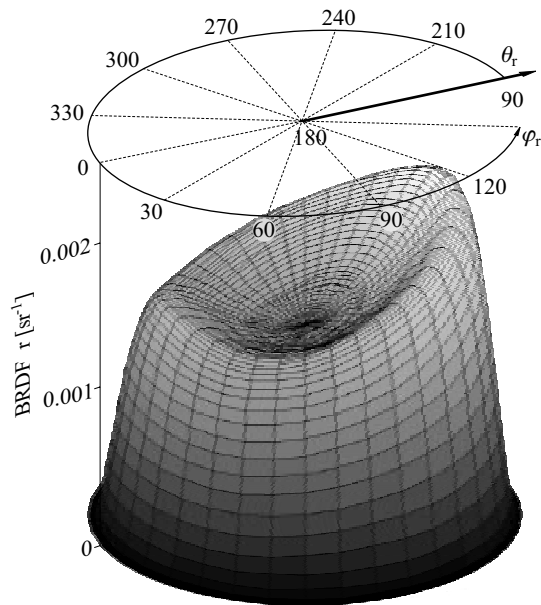


**Fig. 5.** Illustration of the output matrix (the same as in Fig. 4) in cylindrical coordinates

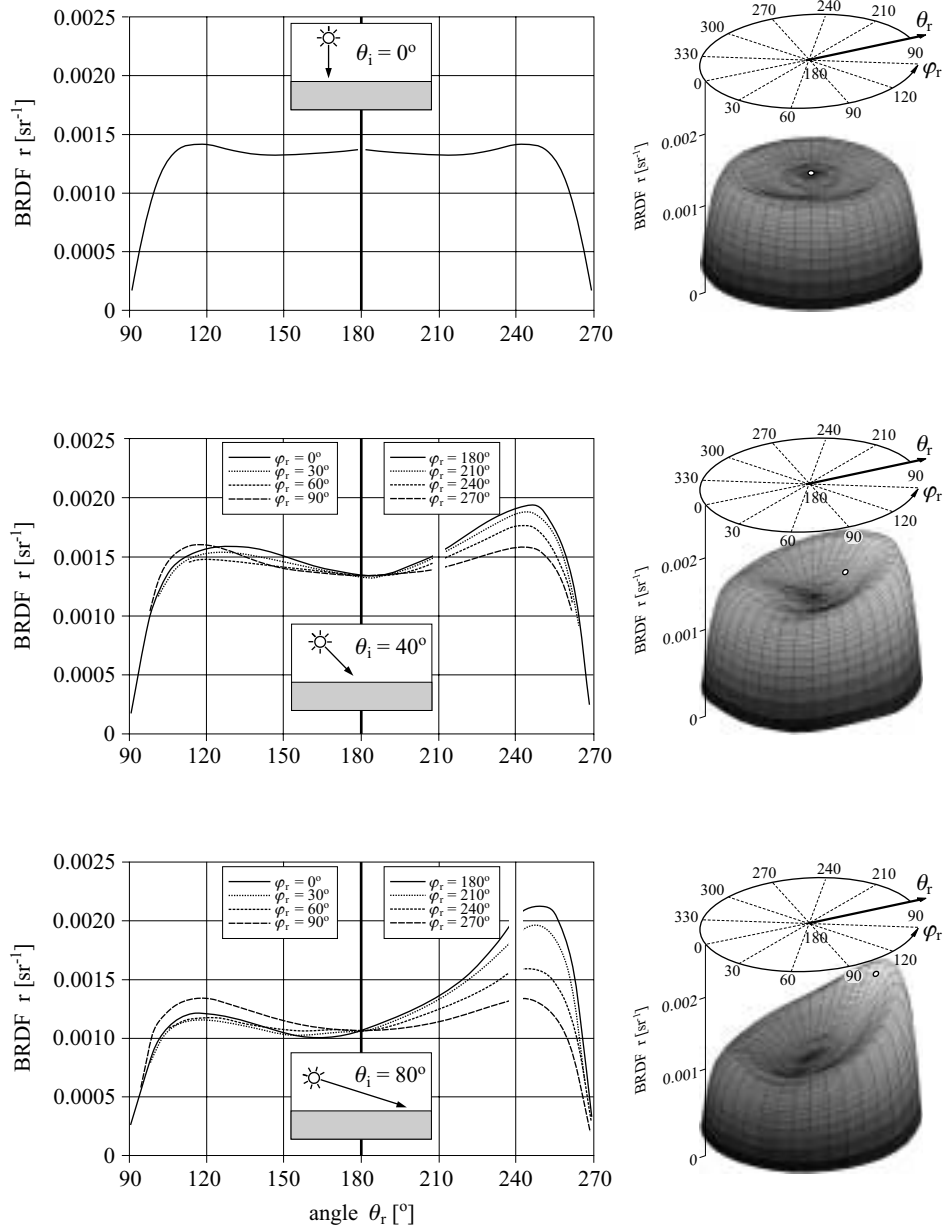


**Fig. 6.** The bidirectional reflectance distribution functions (BRDFs) of a sea area free of oil vs the angle  $\theta_r$  of light reflected in planes incident at the following azimuth angles  $\varphi_r$ :  $0^\circ$  &  $180^\circ$ ,  $30^\circ$  &  $210^\circ$ ,  $60^\circ$  &  $240^\circ$  and  $90^\circ$  &  $270^\circ$  (profiles extracted from BRDFs whose 3D shapes are illustrated on the right-hand side). The upper graphs refer to the angle of solar light incidence  $\theta_i = 0^\circ$ ; middle – to  $\theta_i = 40^\circ$ ; lower – to  $\theta_i = 80^\circ$  (each of three graphs for  $\varphi_i = 0^\circ$ ). The BRDFs relating to specular light have been removed from the graphs

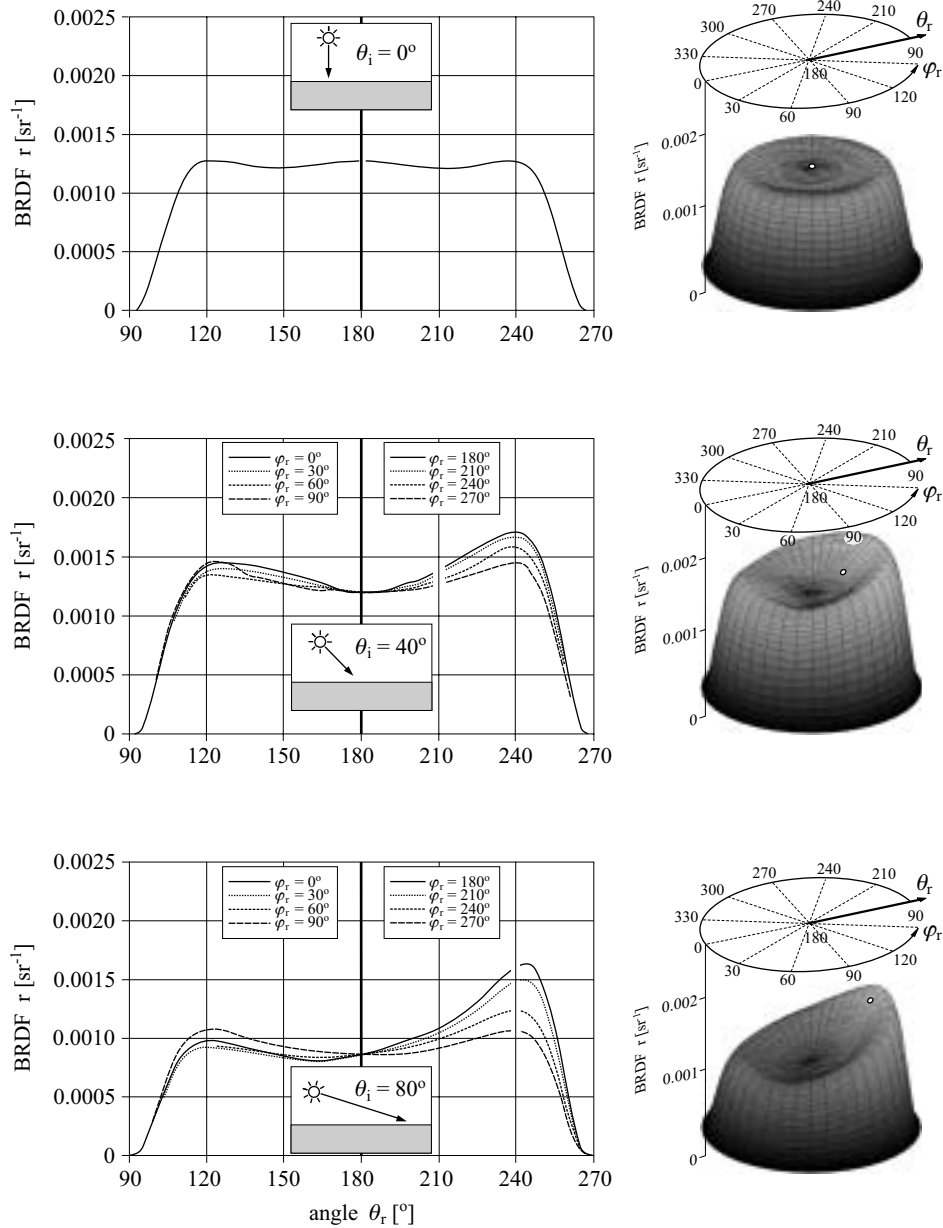


**Fig. 7.** The bidirectional reflectance distribution functions (BRDFs) of a area polluted by an oil film vs the angle  $\theta_r$  of light reflected in planes incident at the following azimuth angles  $\varphi_r$ :  $0^\circ$  &  $180^\circ$ ,  $30^\circ$  &  $210^\circ$ ,  $60^\circ$  &  $240^\circ$  and  $90^\circ$  &  $270^\circ$  (profiles extracted from the BRDFs whose 3D shapes are illustrated on the right-hand side). The upper graphs refer to the angle of solar light incidence  $\theta_i = 0^\circ$ ; middle – to  $\theta_i = 40^\circ$ ; lower – to  $\theta_i = 80^\circ$  (each of three graphs for  $\varphi_i = 0^\circ$ ). The BRDFs relating to specular light have been removed from the graphs



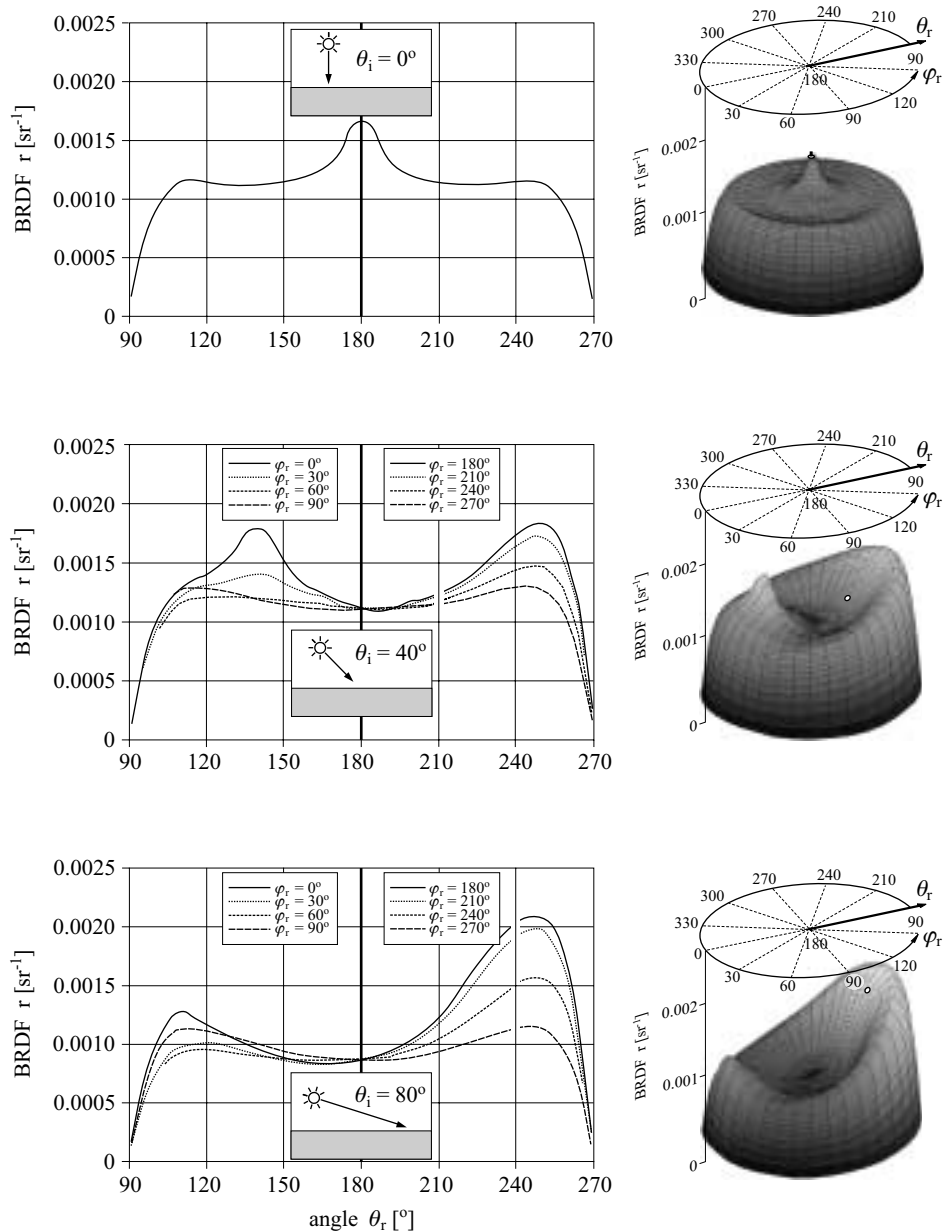


**Fig. 8.** The bidirectional reflectance distribution functions (BRDFs) of a sea area polluted by an oil emulsion vs the angle  $\theta_r$  of light reflected in planes incident at the following azimuth angles  $\varphi_r$ :  $0^\circ$  &  $180^\circ$ ,  $30^\circ$  &  $210^\circ$ ,  $60^\circ$  &  $240^\circ$  and  $90^\circ$  &  $270^\circ$  (profiles extracted from the BRDFs whose 3D shapes are illustrated on the right-hand side). The upper graphs refer to the angle of solar light incidence  $\theta_i = 0^\circ$ ; middle – to  $\theta_i = 40^\circ$ ; lower – to  $\theta_i = 80^\circ$  (each of three graphs for  $\varphi_i = 0^\circ$ ). The BRDFs relating to specular light have been removed from the graphs

Figs 6–8 illustrate these extractions, apart from the three-dimensional shapes of the BRDF on the right-hand sides of the figures. Only selected results of the simulations are represented in the figures: for three angles  $\theta_i$  of solar light incidence –  $0^\circ$ ,  $40^\circ$  and  $80^\circ$ . The graphs in Fig. 6 represent a sea area free of oil, whereas Fig. 7 represents the same area but polluted by an oil film, and Fig. 8 the same area again, but now polluted by an oil emulsion.

### 3. Discussion

It is obvious that both superficial and deep-lying forms of oil, if they occur at high concentrations, radically modify the light conditions above and below the sea surface. On the other hand, the scale of the light field modification caused by low concentrations of oil is interesting. The oil concentrations used in the simulations were relatively low: when the oil film acts as a factor perturbing the light field, the concentration is  $1 \text{ cm}^3$  of oil per  $1 \text{ m}^2$  (thickness  $1 \text{ }\mu\text{m}$ ) of water surface, but when the oil-in-water emulsion is considered, the concentration is  $1 \text{ cm}^3$  of oil in  $1 \text{ m}^3$  of water (1 ppm).

All the BRDFs are plane symmetrical in shape. The plane of symmetry is identical to the plane of solar light incidence. There is only one exception: when sunlight falls perpendicularly on to the sea surface, there is axial symmetry around the perpendicular to the sea surface. There are two BRDF maxima in the plane of light incidence. The first one is situated close to the direction of light incidence, the second in the direction between  $240^\circ$  and  $260^\circ$ . The first maximum is caused by backscattered light, the second one by light entering the atmosphere after single and multiple scattering. The differences between the BRDF for oil-polluted and oil-free areas are shown in Fig. 9. The BRDFs of the area free of oil and that polluted by an oil-film are very similar in shape, whereas the area polluted by the oil emulsion displays a distinct increase in the value of the BRDF near the direction of solar light incidence and a reduction in this value near the perpendicular to the sea surface direction.

It should be mentioned that in current oceanological practice, the quantities describing optical features most commonly measured are apparent optical properties (AOPs) like the remote sensing reflectance  $R_{SR}$  and the radiance reflectance  $R_E$ . Both  $R_{SR}$  and  $R_E$  are measured *in situ*. The values of both  $R_{SR}$  and  $R_E$  depend on the inherent optical properties of water, and there are numerous practical algebraic models of this dependence known to marine optics. If the BRDF and incident solar radiance  $L_i(\theta_i, \varphi_i)$  are

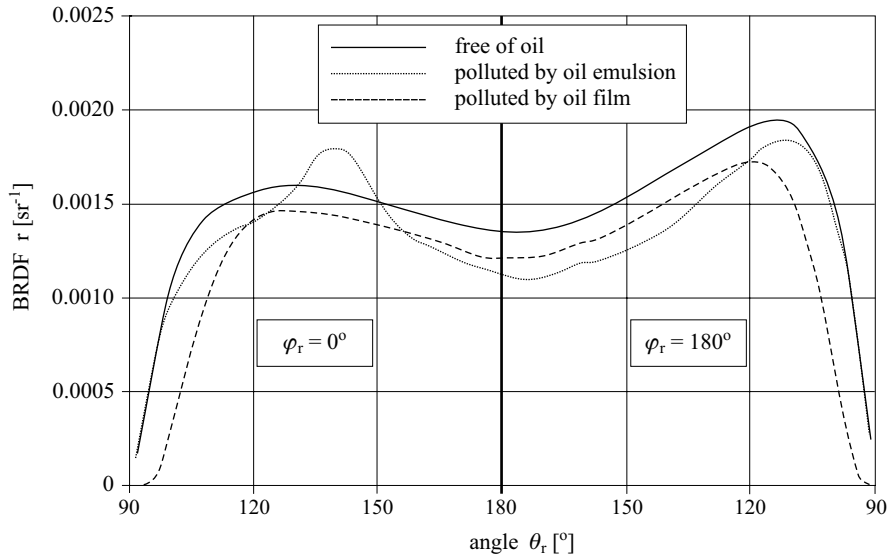


**Fig. 9.** Differentiation of the BRDFs of oil-polluted and oil-free sea areas ( $\theta_i = 40^\circ$ )

known, both the remote sensing reflectance  $R_{SR}$  and the radiance reflectance  $R_E$  can be derived. However, these quantities are of little use unless they are presented in the form of spectral relationships. These spectral relationships of  $R_{SR}$  and  $R_E$  for a sea area polluted by an oil-in-water emulsion are currently being investigated – the preliminary data derived from the BRDF have just been described (Otremba 2004).

Another aspect of BRDF implementation is the directional distribution of the optical contrast of an oil-polluted sea area versus an oil-free one. Two examples of this contrast, derived using eq. (2), are presented in Fig. 10. The first example relates to an oil-in-water emulsion in the sea body, the second, to an oil film on the sea surface.

$$C = \frac{f_{rp} - f_{rc}}{f_{rc}}, \quad (2)$$

where

$f_{rp}$  – BRDF for a polluted sea area,

$f_{rc}$  – BRDF for a sea area free of oil.

Comparing the graphs in Fig. 10, one can see that the directional distribution of contrast for the area polluted by the emulsion is more complicated than for the area polluted by the oil film. It is characteristic that the distribution of contrast for the area polluted by the oil film is axially symmetrical around the perpendicular direction. The contrast is

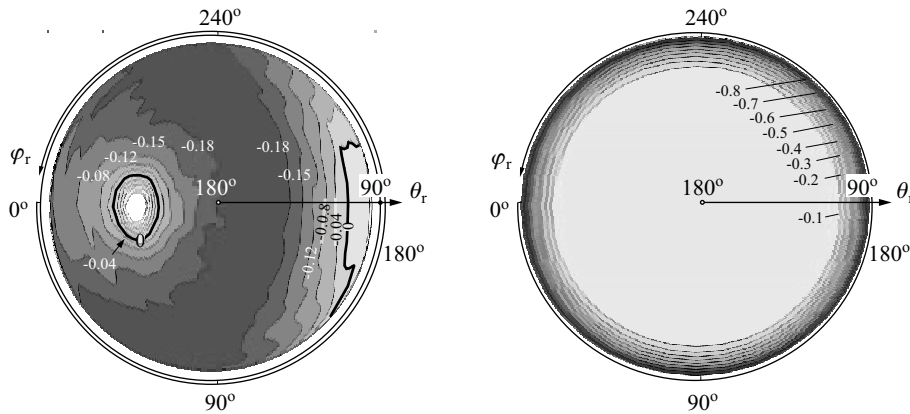


**Fig. 10.** Optical contrast modelled for a sea water surface polluted by an oil-in-water emulsion (left) and by an oil film (right) vs a surface free of oil. The contrast was obtained using the results presented in Figs 6, 7 and 8 for an incident solar light angle of  $40^\circ$

negative at the level  $-0.1$  from the perpendicular direction ( $\theta_r = 180^\circ$ ) to  $\theta_r = 120^\circ$ . For wider angles, the contrast increases rapidly to  $-0.9$ , close to  $\theta_r = 90^\circ$ . On the other hand, the angular distribution of the contrast of the sea area polluted by the oil emulsion is plane symmetrical (like the BRDF). In this case, the contrast of the area polluted by the oil emulsion is negative for a nadir observation ( $-0.18$ ). But a positive peak appears around the direction of solar light incidence, and the contrast reaches a value of  $0.16$ .

The BRDFs presented here relate to selected models of the marine environment (Fig. 1). They indicate the possibility of modelling BRDFs for sea areas polluted by surface or in-water oil substances and also the differences between the shapes of BRDFs for clean and oil-polluted sea areas. Investigations into the influence of sea surface roughness and of the inherent optical properties (IOPs) on the above-water radiance field and on the BRDF are being continued. For surface waves, the preliminary results have been published by Otremba (2002). The roughness factor can be tested relatively easily for in-water pollution using e.g. the Cox-Munk distribution (Cox & Munk 1954); however, for surface oil films, this problem is more complicated (because questions arise relating to the impact of an oil-film on the wave slope distribution).

Although the BRDF modelling process described in this paper relates to oil, other substances can be treated analogously, with extension to other wavelengths. Regardless of whether one takes into consideration natural components of sea water like plankton, microbes or air bubbles,

or external substances like sand-dusts, their inherent optical properties – their absorption coefficients, scattering coefficients and phase functions of those substances – should be established.

### Acknowledgements

The author would like to express his gratitude to Dr. Jacek Piskożub of IO PAS for providing the basic Monte Carlo code which, after adaptations, was applied in the study described in this paper.

### References

- Cox C., Munk W. H., 1954, *Measurements of the sea surface from photographs of the sun's glitter*, J. Opt. Soc. Am., 44(11), 838–850.
- HELCOM, 1991, *Airborne surveillance with remote sensing equipment in the Baltic Sea area*, HELCOM Recommendation 12/8 – adopted 20 February 1991 having regard to article 13, paragraph b) of the Helsinki Convention, [<http://www.helcom.fi/recommendations/rec12.8.html>].
- HELCOM, 2002, *Location of oil spillages observed by aerial surveillance within the North and Baltic Sea areas in 2002*, [<http://www.helcom.fi/sea/oilbsns2002.pdf>].
- Liang S., Strahler A., 1999, *Summary of the international forum on BRDF*, The Earth Observer, 11, 27 pp.
- Martonchik J. V., Bruegge C. J., Strahler A. H., 2000, *A review of reflectance nomenclature used in remote sensing*, Remote Sens. Rev., 19, 9–20.
- Mobley C. D., Zhang H., Voss K. J., 2003, *Effects of optically shallow bottoms on upwelling radiances: Bidirectional reflectance distribution function effects*, Limnol. Oceanogr., 48(1, part 2), 337–345.
- Nicodemus F. E., 1963, *Radiance*, Am. J. Phys., 31(5), 368–377, [repr. in:] *Selected papers on radiometry*, I. J. Spiro (ed.), SPIE Milestone Ser., Vol. MS14 (1990), pp. 74–83, Bellingham, WA, 704 pp.
- Nicodemus F. E., 1970, *Reflectance nomenclature and directional reflectance and emissivity*, Appl. Optics, 9(6), 1474–1475.
- Nicodemus F. E., Richmond J. C., Hsia J. J., Ginsberg I. W., Limperis T., 1977, *Geometrical considerations and nomenclature for reflectance*, NBS Monograph 160, Natl. Bureau of Standards, Washington, DC, 52 pp.
- NRC (U. S. National Research Council), 2003, *Oil in the sea III: Inputs, fates, and effects*, Natl. Acad. Press, Washington, DC, p. 280.
- Otremba Z., 2000, *The impact on the reflectance in VIS of a type of crude oil film floating on the water surface*, Opt. Express, 7(3), 129–134.

- Otremba Z., 2002, *Simulation of the contrast of the sea areas polluted by oil spilled on the surface and dispersed in the water column*, [in 44th thematic issue:] *Boundary field problems and computer simulation*, Sci. Proc. Riga Tech. Univ., Ser. Computer Science, 12, 6–12, [[http://www.rtu.lv/www\\_emc/emc\\_home.htm](http://www.rtu.lv/www_emc/emc_home.htm)].
- Otremba Z., 2004, *Influence of oil dispersed in seawater on the bi-directional reflectance distribution function (BRDF)*, Opt. Appl., (accepted).
- Otremba Z., Piskozub J., 2004, *Phase functions of oil-in-water emulsions*, Opt. Appl., 34 (1), 93–99.
- Petzold T., 1977, *Volume scattering functions for selected ocean waters*, [in:] *Light in the sea*, J. E. Tyler (ed.), Dowden, Hutchinson & Ross, Stroudsburg, PA, 152–174.
- Schaaf C. B., Gao F., Strahler A. H., Lucht W., Li X., Tsang T., Strugnell N. C., Zhang X., Jin Y., Muller J., Lewis P., Barnsley M., Hobson P., Disney M., Roberts G., Dunderdale M., Doll C., d'Entremont R., Hu B., Liang S., Privette J., Roy D., 2002, *First Operational BRDF, albedo and nadir reflectance products from MODIS*, Remote Sens. Environ., 83 (1)–(2), 135–148.